Mechanism of Ribonucleic Acid Chain Initiation. 2. A Real Time Analysis of Initiation by the Rapid Kinetic Technique†

Nobuo Shimamoto and Cheng-Wen Wu*

ABSTRACT: Rapid kinetic studies on the initiation of RNA synthesis catalyzed by *Escherichia coli* RNA polymerase were performed by using a multimixing stopped-flow apparatus. Tritium-labeled UTP was first mixed with a preincubated mixture of enzyme, template poly(dA-dT), and initiator UpA to form UpAp[^{3}H]U. After a selected time interval, the reaction mixture was mixed with a third solution containing unlabeled UTP and ATP to allow the elongation of poly(rA-rU). The net [^{3}H]UMP incorporation into acid-precipitable product measures the formation of the initiation complex which has subsequently been elongated in RNA chains without enzyme turnover. The time course of formation of the initiation complex thus measured is biphasic with a time lag of about 30 ms and a plateau after 0.5 s. The kinetic data could be analyzed by a two-exponential equation, giving two relaxation times of about 40 and 100 ms. The presence of time lag and the apparent lack of dependence of the two relaxation times on the concentrations of UpA and [^{3}H]UTP indicate that an inactive intermediate is formed after substrate binding to the enzyme–template complex via a rapid equilibration. This inactive intermediate is then converted into an active initiation complex. In contrast, the total relaxation amplitude shows a strong dependence of [^{3}H]UTP concentration in a manner suggesting that more than one UTP molecule is bound to the enzyme–DNA complex during the initiation process. Based on kinetic arguments, it is proposed that the inactive intermediate is formed from the enzyme–DNA–UpA–UTP complex and converted into the enzyme–DNA–UpApU complex. Moreover, the additional UTP molecule may bind to the latter complex or the inactive intermediate mentioned above. Two minimal mechanisms of the initiation of RNA synthesis consistent with all the data are presented.

RNA synthesis catalyzed by DNA-dependent RNA polymerase can be divided into several processes (Goldthwait et al., 1970): (a) binding of the enzyme to the DNA template, (b) initiation of RNA synthesis, (c) elongation of the RNA chain, and (d) termination of the RNA synthesis. Attempts to study these individual processes by steady-state kinetics have not been fruitful due to the complexity of these processes. By means of a non-steady-state approach (Shimamato & Wu, 1980), we have determined the order of substrate binding in RNA chain initiation and measured the number of active RNA polymerase–DNA complexes. In addition, kinetic evidence was also presented to indicate that more than one UTP molecule was bound to the RNA polymerase–poly(dA-dT) complex during the initiation step of RNA synthesis.

Some important questions immediately follow. How fast are the substrate binding steps? What are the other elementary steps involved in the initiation process? Which is the rate-determining step? The answers to these questions are necessary to establish the molecular mechanism of RNA chain initiation. In order to obtain this mechanistic information, it is essential to resolve the initiation process into its elementary steps on the time axis by using rapid kinetic techniques. We report here the first real time measurements of RNA chain initiation by a fast kinetic technique. These measurements are based on a method developed in the preceding paper (Shimamato & Wu, 1980) to observe the formation of the initiation complex which is subsequently elongated into RNA chain without enzyme turnover. Two minimal mechanisms of the RNA chain initiation consistent with the data are discussed.

Materials and Methods

Materials. All materials used are the same as those described in the preceding paper (Shimamoto & Wu, 1980).

Methods for Rapid Kinetic Experiments. (1) Multimixing Apparatus. Figure 1 shows a schematic illustration of the multimixing apparatus used in this study. The apparatus contains three sample syringes (A, B, and C), two mixing jets (1 and 2), a collecting syringe, and a waste syringe. Solutions A and B are mixed first as jet 1. The product of this first reaction is "aged" for a time interval of 20 ms–10 s by passing through a delay line and then mixed with an equal quantity of solution C at jet 2. To ensure collection of freshly reacted materials, we purged part of the final reaction mixture into the waste syringe before it is driven into the collection syringe. The reaction time, which is the length of time required for the reactants to travel from jet 1 to jet 2, is controlled by the flow speed and the length of the delay line (continuous mode). For a reaction time longer than 180 ms, the operation becomes impractical due to excessive length of the delay line and the large purge volume and residual. For minimization of the waste of materials, the flow is stopped for a variable time interval after the purging and resumed again by closing and opening of a solenoid valve (interrupted mode). The total volume of reaction mixture needed in each run equals to the sum of the volume purged into the waste syringe, V_p, and the volume collected in the collection syringe, V_c.

(2) Reaction System. The experimental system used in the rapid kinetic studies was a kind of pulse–chase experiment identical with system C in the preceding paper (Shimamoto & Wu, 1980), which consisted of three steps: (a) preincubation of RNA polymerase, poly(dA-dT), and initiator UpA[1] in syringe A to form the enzyme–DNA–initiator complex

$$\text{RPase} + \text{poly(dA-dT)} \rightleftarrows \text{E} \overset{\text{UpA}}{\rightleftharpoons} \text{E·UpA} \qquad (1)$$

† From the Department of Biochemistry, Albert Einstein College of Medicine, Bronx, New York 10461. *Received March 5, 1979.* This work was supported in part by Research Grants GM 19062 from the National Institutes of Health and BC 94 from the American Cancer Society.

* Correspondence should be addressed to this author. He is the recipient of the Irma T. Hirschl Scientific Cancer Award.

[1] Abbreviations used: UpA, uridylyl(3′–5′)adenosine; ApUpA, adenylyl(3′–5′)uridylyl(3′–5′)adenosine; UpApU, uridylyl(3′–5′)adenylyl-(3′–5′)uridine.

0006-2960/80/0419-0849$01.00/0

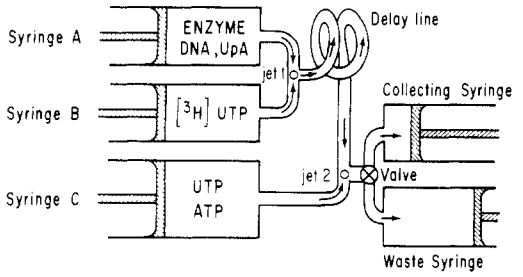

FIGURE 1: Schematic illustration of a multimixing apparatus. A typical combination of the reactants in three sample syringes is also shown.

where E is the enzyme–poly(dA-dT) complex and E·UpA is the enzyme–DNA–initiator complex, (b) mixing of the enzyme–DNA–initiator complex in syringe A and radioactively labeled UTP in syringe B at jet 1 to form the labeled initiation complex E·UpApU

$$\text{E·UpA} + \text{UTP*} \rightleftarrows \underset{\text{UTP*}}{\text{E·UpA}} \rightleftarrows \text{E·UpApU*} + \text{PP}_i \quad (2)$$

where the asterisk denotes the radioactive label, and (c) mixing of the initiation complex with unlabeled ATP and UTP (in syringe C) at jet 2 to elongate the poly(rU-rA) chain

$$\text{E·UpApU*} \xrightarrow{\text{UTP, ATP}} \text{E·UpApU*pApU'pApU'} \ldots \quad (3)$$

In this step, the concentration of ATP was limited (4 μM) to minimize the turnover of enzyme during elongation, while the concentration of unlabeled UTP was 2–4 orders of magnitude higher (6.13 mM) than that of [^{3}H]UTP in syringe B to dilute out the specific activity of the latter so that the incorporation of [^{3}H]UMP into poly(rU-rA) was greatly reduced due to its low specific activity (as indicated by U′ in contrast to the high specific activity U*). The small quantity of [^{3}H]UMP incorporation during elongation and the possible complication of enzyme turnover were corrected by a control experiment in which unlabeled UTP was placed in syringe B whereas in syringe C [^{3}H]UTP was added to produce the same amount of [^{3}H]UMP incorporation during the elongation period as in the original experiment. By subtraction of the control value, the net incorporation of [^{3}H]UMP into poly(rU-rA) would represent the measure of the initiation complexes formed which were subsequently elongated into RNA chains without enzyme turnover [see Schimamoto & Wu (1980)].

(3) Experimental Procedures. Nitrogen gas at 18–30 psi was used to drive the plungers of the multimixing apparatus. At pressures higher than this range, poly(dA-dT) appeared to be sheared hydrodynamically as indicated by a significant increase in the end-addition reaction (Nath & Hurwitz, 1974). The dead time of the apparatus at this pressure range was about 20 ms. The delay lines used were polyethylene tubing of 2, 6, 10, and 12 in. long with a unit capacity of 17 μL/in. All flow channels, including the sample syringes and the delay lines but not the collection and waste syringes, were immersed in a constant temperature water bath at 37 °C. A 1-mL glass syringe was used for collection and a 5-mL plastic syringe was used for waste. The temperature of the collection syringe was maintained at 37 °C by a thermostated air flow.

To start an experiment, we first filled all the sample syringes with distilled water. A delay line was installed, the nitrogen gas pressure was set, and the time durations of purging and collection were adjusted to obtain selected values of the reaction time, V_p, and V_c. The flow channels were flushed with distilled water as much as possible to remove residual reactants remaining from the previous run. This procedure was essential

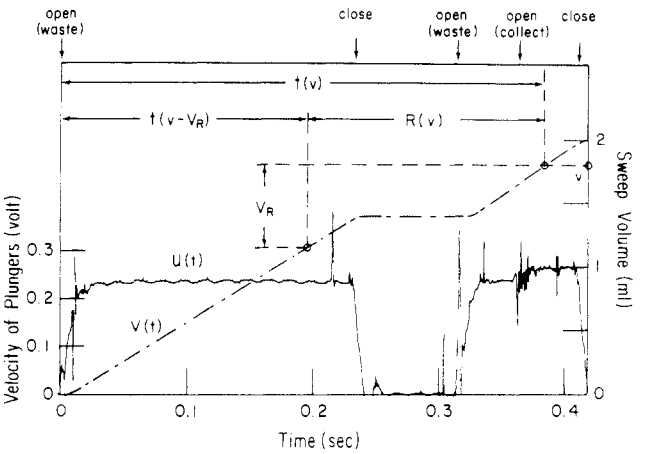

FIGURE 2: Determination of the reaction time in the interrupted mode. The curve $U(t)$ is the velocity of plungers as recorded on a transient recorder in a typical run. The spikes in the velocity data were due to electric noise from solenoids and mechanical collision between the ram and plungers. By approximation of polygons with vertices at (0, 0) (0.018, 0.235), (0.230, 0.235), (0.240, 0), (0.312, 0) (0.332, 0.242), (0.360, 0.242), (0.362, 0.150), (0.407, 0.270), and (0.417, 0), $U(t)$ was integrated and normalized to give the sweep volume with respect to time, $V(t)$. In this run, values of V_c and V_p were measured to be 0.38 and 1.62 mL, respectively. The value of V_R was 0.64 mL. The reaction time was calculated to be 189 ± 2 ms. The relationships among $t(v)$, $t(v - V_R)$, $R(v)$, and V_R are also illustrated for an arbitrary value of sweep volume v.

for good reproducibility. The samples were then introduced into the sample syringes and the flow was activated. Immediately after the run, the value of V_c was read from the collecting syringe and the reaction mixture was transferred into a test tube. After incubation for 2 min at 37 °C, 20 volumes of cold, 5% trichloroacetic acid was added to the mixture to precipitate the RNA product. The procedures for filtration of acid-insoluble materials by glass-fiber filters and for determination of radioactivity incorporations by scintillation counting were the same as those described in the preceding paper (Shimamoto & Wu, 1980). Because the value of V_c varied in each run, it was more convenient to express the incorporation of [^{3}H]UMP in concentration rather than in absolute amount.

The flow rate was measured by a velocity transducer attached to the actuator which drove the plungers of the sample syringes and was recorded on a Biomation 802 transient recorder. The value of V_p was read from the waste syringe.

(4) Determination of the Reaction Time. In principle, the reaction time, R, is obtained by dividing the volume of the channel between the two jets with the flow velocity. However, a reliable determination of the reaction time cannot be done due to the mechanical delay during activation of the plungers and during opening and closing of the solenoid valves. We have developed a very accurate method for such determination: the reaction time for each small part of the sample in the collection syringe was determined, from which an average value of R for the whole sample was calculated.

A typical example of a run in the interrupted mode is illustrated in Figure 2. The velocity of plungers recorded on the time axis, $U(t)$, reflects the opening and closing of the solenoid valves during the run. This curve can be integrated to a volume function

$$V(t) = C_0 \int_0^t U(\tau)\, d\tau \quad (4)$$

where C_0 is the flow rate constant of the apparatus [2.7 ± 0.1 mL/(V s)]. The function $V(t)$ represents the sweep volume from the sample syringes at time t. At the end of the run, the

total sweep volume should be equal to the sum of the purge and collected volume, $V_p + V_c$. Thus, the value of C_0 can be determined from eq 4 by using the relation $V(\infty) = V_p + V_c$.

Let us consider a thin layer of solution perpendicular to the direction of flow which travels along the flow channel and reaches jet 2 at time t. The sweep volume, v, of this layer of solution from time zero to t is equal to $V(t)$. Since the final sweep volume is $V_p + V_c$, this layer of solution can enter the collecting syringe only when the sum of v and the volume between jet 2 and the inlet of the collecting syringe v' (=50 μL, a machine constant) is smaller than $V_p + V_c$. On the other hand, if the sum of v and v' is smaller than the purge volume, V_p, it will either enter the waste syringe or remain at a position between jet 2 and the inlet of the waste syringe. Thus, for this layer of solution to be collected in the collection syringe, the following conditions must be fulfilled:

$$(V_p - v') < v < (V_c + V_p - v') \quad (5)$$

The reaction time for the layer of reaction mixture, $R(v)$, which is defined as the time required to travel from jet 1 to jet 2, is related to the reaction channel volume, V_R, as shown in Figure 2. V_R is actually twice the channel volume from jet 1 to jet 2 because the output volume of jet 2 doubles due to mixing with the solution from syringe C. As can be seen from Figure 2, if $V(t)$ is expressed by its inverse function $t(V)$, then

$$R(v) = t(v) - t(v - V_R) \quad (6)$$

The reaction time of the reaction mixture collected can now be derived by averaging $R(v)$ over all layers of the solution entered the collection syringe as described by

$$R = \frac{1}{V_c}\int_{V_p-v'}^{V_c+V_p-v'} R(v)\, dv \quad (7)$$

The mean-square error, ϵ^2, involved in the value of reaction time determined according to eq 7 can be estimated by

$$\epsilon^2 = \frac{1}{V_c}\int_{V_p-v'}^{V_c+V_p-v'} [R(v) - R]^2\, dv \quad (8)$$

The value of ϵ^2 is indicative of the quality of each run.

(5) *Analysis of Kinetic Data.* Because the reaction time was calculated after each run, it was not possible to carry out a control experiment for each run with exactly the same reaction time. Nonetheless, since most of the [^{3}H]UMP incorporation in the control system occurred during the 2-min elongation step (step 3), one would expect that it should show little dependence on the reaction time (step 2). In fact, the experimental value of [^{3}H]UMP incorporation in the control system for the reaction time of 0.04 s was found to agree well with that observed for the reaction time of 0.5 s or longer as measured by manual mixing experiments. The time course of the net [^{3}H]UMP incorporation observed in a multimixing experiment was biphasic (see the text) and was analyzed by a two-exponential equation

$$\text{net [}^3\text{H]UMP incorporated} = A_1 \exp(-t/\tau_1) + A_2 \exp(-t/\tau_2) + B \quad (9)$$

with two relaxation times τ_1 and τ_2 and three amplitude constants A_1, A_2, and B. A nonlinear least-squares method was used to fit the kinetic data to eq 9. In order to minimize the number of independent variables in the fitting procedures, it was assumed that at time zero the initial velocity of the net [^{3}H]UMP incorporation was zero and thus

$$A_2 = -\frac{\tau_1}{\tau_2}A_1 \quad (10)$$

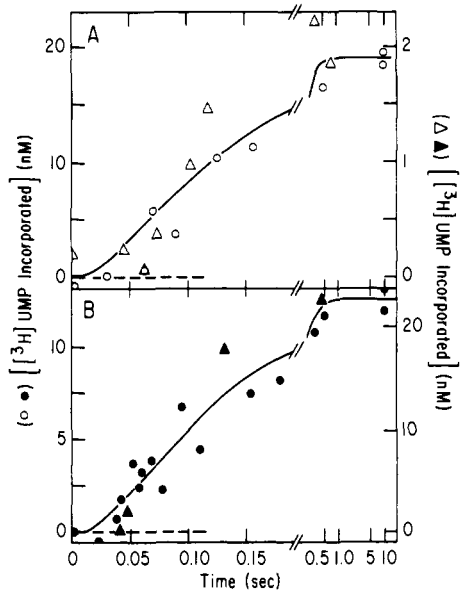

FIGURE 3: Time course of the net incorporation of the first UMP into poly(rA-rU) at various concentrations of UTP. The reaction mixture contained RNA polymerase holoenzyme (100 μg/mL), poly(dA-dT) (35 μM in nucleotide), 50 μM UpA (after first mixing) and UTP in 50 mM Tris-HCl (pH 7.9), 100 mM KCl, 10 mM $MgCl_2$, and 0.2 mM dithiothreitol. The concentration of [^{3}H]UTP present after the first mixing was as follows: (A) 100 μM (○) and 10.8 μM (△); (B) 50 μM (●) and 400 μM (▲).

Table I: Best Fit Parameters of the Kinetic Data Presented in Figure 3 According to Equation 9

concn (μM)		relaxation times (ms)		total amplitude (nM)
UpA	UTP	τ_1	τ_2	$A_1 + A_2$
50	10.8	40.0	91	2.0
50	50	43.5	111	12
50	100	43.5	100	20
5.0	100	40.8	87	7.0

Results

Figure 3 shows the time course of the net [^{3}H]UMP incorporation into poly(rA-rU) catalyzed by RNA polymerase in the multimixing experiments with four different [^{3}H]UTP concentrations. In all cases, there exist a time lag of about 30 ms and a plateau after 0.5 s. The time lag in a biphasic kinetic curve can, in principle, be approximated by two exponential processes with amplitudes of opposite sign. Since two forms of an enzyme with different activity will produce two relaxation amplitudes with the same sign, the observed time lag cannot be explained by the heterogeneity of the enzyme. It will, however, reflect the existence of at least two steps in the experimental time region. By means of a nonlinear least-squares analysis, the data were fit to eq 9 and the best fit parameters are listed in Table I. When the UTP concentration was varied from 10 to 100 μM at a constant concentration of UpA, the total amplitude increased 1 order of magnitude but the relaxation times, τ_1 and τ_2, remained unchanged. A similar phenomenon was observed as the concentration of UpA was varied while that of UTP was held constant. These common features enabled the time courses at different UTP and UpA concentrations to be superimposed simply by adjusting the scale of the ordinate as presented in Figure 3.

The observation that the relaxation times are independent of the UTP concentration suggests that UTP binding to the enzyme–poly(dA-dT) complex was in a rapid equilibrium,

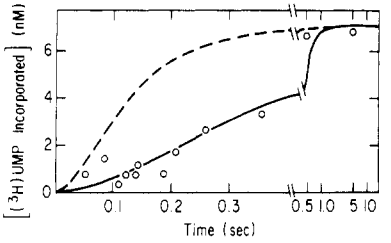

FIGURE 4: Time course of the net incorporation of the first UMP into poly(rA-rU) catalyzed by core RNA polymerase. The experimental conditions were essentially identical with those in Figure 3 except that the core enzyme was used and [UTP] = 100 μM.

Table II: Comparison of the Two Relaxation Times Observed with Core and Holoenzyme

enzyme preparation[a]	τ_1 (ms)	τ_2 (ms)
holoenzyme	43.5	100
core enzyme	178	243

[a] The holoenzyme preparation had a σ subunit content of about 70%. The concentration of UpA was 50 μM and that of UTP was 100 μM in these experiments.

probably faster than the mixing time of the multimixing apparatus (20 ms). For the experiments shown in Figure 3, the initiator UpA was preincubated with the enzyme–poly(dA-dT) complex in syringe A prior to mixing with [^{3}H]UTP in syringe B. When UpA was deleted from syringe A and, instead, placed in syrine B together with [^{3}H]UTP, no apparent alteration in the time course of net [^{3}H]UMP incorporation was observed. Furthermore, the two relaxation times associated with the net [^{3}H]UMP incorporation in these experiments did not change significantly by lowering the concentration of UpA from 50 to 5 μM (Table I). These results clearly indicate that UpA binding to the enzyme–poly(dA-dT) complex was also in rapid equilibrium and was faster than the two relaxations observed experimentally.

Multimixing experiments were also performed with core polymerase under similar conditions. As shown in Figure 4, the time course of the net [^{3}H]UMP incorporation is again biphasic with a time lag of about 100 ms, and the observed relaxation times were 2–4 times longer than those observed with holoenzyme (Table II). The total amplitude of the net [^{3}H]UMP incorporation is about 1/3 of that obtained with the same concentration of holoenzyme. It should be pointed out that the holoenzyme preparation used in these studies contained about 30% of core polymerase. Given that the holoenzyme is 2–4 times more efficient than the core enzyme in initiating the poly(dA-dT)-directed RNA synthesis (Figures 3 and 4), the amount of core enzyme present in the preparation used for Figure 3 would account for the net [^{3}H]UMP incorporation of no more than about 10% of that observed in total.

Discussion

Simplest Mechanism for Initiation of RNA Synthesis. In the multimixing experiments presented here, the net incorporation of [^{3}H]UMP into the acid-precipitable material measures the formation of initiation complexes (E·UpApU*) which are subsequently elongated into RNA chains without enzyme turnover [cf. system C in Schimamoto & Wu (1980)]. The most important observations in these fast kinetic measurements are the existence of a lag phase in the time course of the net [^{3}H]UMP incorporation and the apparent independence of the two relaxation times associated with the initiation process with respect to the concentrations of initiator

Scheme I: Simplest Mechanism Involved in RNA Chain Initiation and Possible Positions of Additional Intermediates[a]

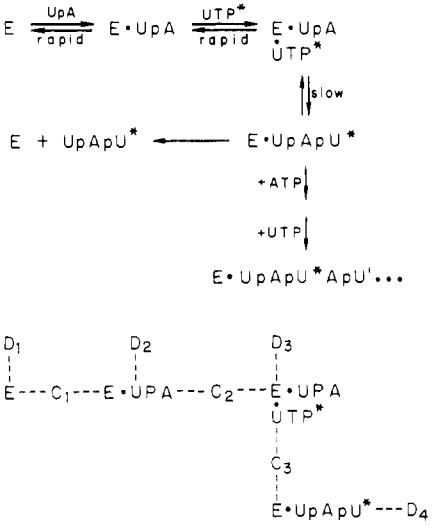

[a] The enzyme–poly(dA-dT) complex is denoted as E, a dead-end intermediate as D_i, and a central intermediate as C_i. The asterisk denotes labeled compounds with high specific activity and the apostrophe denotes those diluted with unlabeled compounds.

and substrate. On the basis of these observations, one may eliminate mechanisms in which the initiator or substrate binding is participating in the steps corresponding to the relaxation times observed. In such cases, either increasing or decreasing substrate concentration would alter the rates of association steps in the binding and thereby change the relaxation times significantly.

The simplest mechanism for RNA chain initiation is illustrated in Scheme I. The sequence of binding of the first two substrates in the poly(dA-dT)-directed DNA synthesis has been demonstrated in the preceding paper (Shimamoto & Wu, 1980). The initiator UpA binds first to the enzyme–poly(dA-dT) complex, followed by binding of UTP*. After these binding steps, there will be the formation of the first phosphodiester bond, producing the initiation complex E·UpApU*. The UpApU* formed could either be released from the enzyme–poly(dA-dT) complex (abortive initiation) or elongated into poly(rA-rU) after addition of unlabeled ATP and UTP (productive initiation). The time course of the net UMP* incorporation shown in Figure 3 reflects the kinetics of the formation of the initiation complex which is ready for elongation.

Requirement for an Additional Intermediate. The mechanism presented in Scheme I is oversimplified since it gives only a single relaxation time in the experimental time region corresponding to the step of the phosphodiester bond formation. Therefore, more intermediates must be involved in the initiation process. There are seven possible positions that an additional intermediate can be located: four dead-end intermediates (D_1–D_4) and three central intermediates (C_1–C_3). These positions are also given in Scheme I. If the rates of conversion of these intermediates from their precursors are comparable to the observed relaxation rates (slower than the substrate binding steps), the addition of any one of the seven intermediates to the mechanism would give two relaxation times.

An attempt was made to resolve these seven possibilities by a phenomenological treatment (Shimamoto, 1976) which reduces all the possible mechanisms into three generalized two-step mechanisms (Scheme II). In this treatment, all enzyme complexes in rapid equilibrium are grouped into one

Scheme II: Generalized Two-Step Mechanisms Deduced by a Phenomenological Treatment[a]

generalized mechanism	intermediate involved	
$D^* \underset{k_{-1}^*}{\overset{k_1^*}{\rightleftharpoons}} E^* \underset{k_{-2}^*}{\overset{k_2^*}{\rightleftharpoons}} T^*$	D_1, D_2, D_3	(a)
$E^* \underset{k_{-2}^*}{\overset{k_2^*}{\rightleftharpoons}} T^* \underset{k_1^*}{\overset{k_{-1}^*}{\rightleftharpoons}} D^*$	D_4	(b)
$E^* \underset{k_{-1}^*}{\overset{k_1^*}{\rightleftharpoons}} C^* \underset{k_{-2}^*}{\overset{k_2^*}{\rightleftharpoons}} T^* \xrightarrow{k_3^*}$	C_1, C_2, C_3	(c)

contents of quasi-intermediates

intermediate	E*	D* or C*	T*
D_1	E, E·UpA, E·UpA·UTP	D_1	E·UpApU
D_2	E, E·UpA, E·UpA·UTP	D_2	E·UpApU
D_3	E, E·UpA, E·UpA·UTP	D_3	E·UpApU
D_4	E, E·UpA, E·UpA·UTP	D_4	E·UpApU
C_1	E	C_1, E·UpA, E·UpA·UTP	E·UpApU
C_2	E, E·UpA	C_2, E·UpA·UTP	E·UpApU
C_3	E, E·UpA	C_3, E·UpA·UTP	E·UpApU

[a] The effective rate constant k_3^* is associated with the release of UpApU from the initiation complex E·UpApU. This step is included in k_{-2}^* in mechanisms a and b.

"quasi-intermediate". The quasi-intermediates containing the free enzyme–DNA complex, the dead-end intermediate, the central intermediate, and the initiation complex (E·UpApU) are designated as E*, D*, C*, and T*, respectively. The contents of these quasi-intermediates are also listed in Scheme II. The k_i^* values are introduced to denote the effective rate constants associated with the interconversions of the quasi-intermediates (details are given in the Appendix). When UpA and UTP are in excess of the enzyme, the relative populations of the enzyme complexes in a quasi-intermediate are constant in the time scale concerned because they are in rapid equilibria. The effective rate constants, however, are dependent on the concentration of UpA and UTP. In all three generalized mechanisms shown in Scheme II the following relationships can be derived for the two relaxation times (see Appendix):

$$\frac{1}{\tau_1}\frac{1}{\tau_2} = k_1^* k_2^* [E]_0 / [T^*]_\infty \tag{11}$$

$$\frac{1}{\tau_1} + \frac{1}{\tau_2} = k_1^* + k_{-1}^* + k_2^* + k_{-2}^* \ (+k_3^*) \tag{12}$$

where $[E]_0$ is the total enzyme concentration and $[T]_\infty$ is the stationary concentration of the initiation complex capable of elongation.

For the mechanisms containing the dead-end intermediates (type D mechanism), the initial velocity of the formation of T* at the saturation concentrations of UpA and UTP can be expressed as

$$V_0 = \left.\frac{dT^*}{dt}\right|_{t=0} = k_2^* [E^*]_{t=0} = k_2 [E]_0 \tag{13}$$

since $[E]_0 = [E^*] + [D^*] + [T^*]$ and $[D^*]$ and $[T^*]$ approach zero at $t = 0$. Equation 13 is inconsistent with the observation of a lag phase (Figure 3) since it requires that V_0 and, hence, k_2 approach zero. Furthermore, from eq 11 and 13, one can obtain

$$\frac{[T^*]_\infty}{V_0} = k_1^* \tau_1 \tau_2 \tag{14}$$

In Figure 3, $[T^*]_\infty$ is the plateau level and V_0 is the slope of the net UMP incorporation at $t = 0$. Thus, the value of $[T^*]_\infty / V_0$ can be obtained from the time coordinate at which the initial slope intersects at the plateau level. The value

Scheme III: Type C Mechanisms

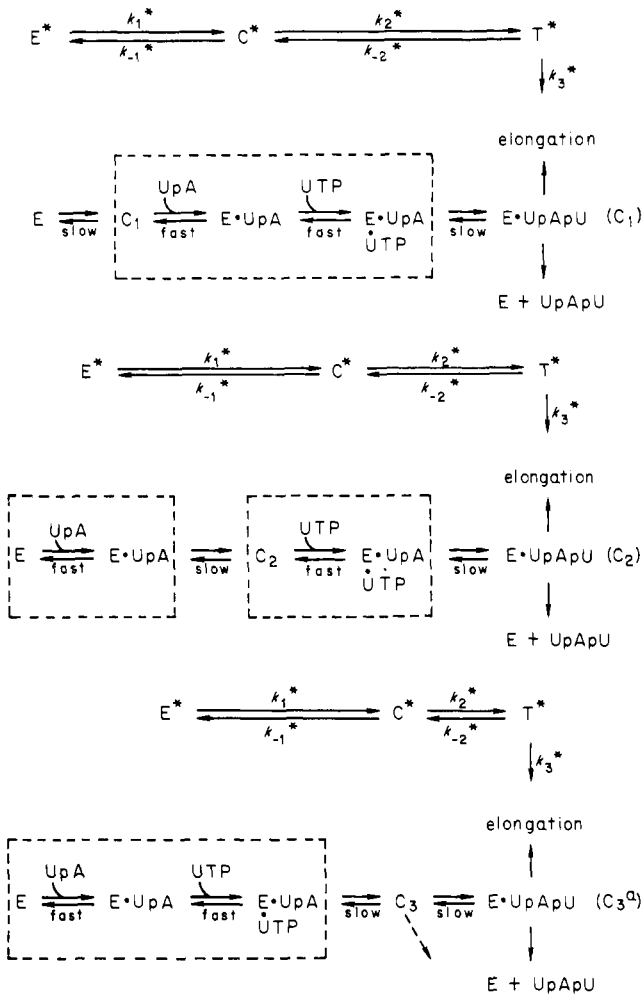

[a] In the C_3 mechanism, the formation of the phosphodiester bond may be completed at C_3 or the intermediate that follows (see the text). In the former case, the release of UpApU from C_3 is shown by an arrow with dashed line.

obtained is much longer than the sum of τ_1 and τ_2 (0.15 s). It follows that

$$k_1^* \tau_1 \tau_2 \gg \tau_1 + \tau_2$$

thus

$$k_1^* \gg \frac{1}{\tau_1} + \frac{1}{\tau_2} \tag{15}$$

This relationship is inconsistent with eq 12. Kinetically it means that the type D mechanisms cannot account for the observed time lag (small V_0) and, hence, can be excluded.

Scheme III shows the three type C mechanisms. The mechanism C_1 can be ruled out based on the same argument used for the type D mechanisms, because when an excess of UpA was preincubated with the enzyme–DNA complex, the initial velocity of the formation of T* can also be described by eq 13. The situation for the C_2 mechanism is more complex. If $k_1^* \gtrsim k_{-1}^*$, the preincubation of UpA with the enzyme–DNA complex should shift the equilibrium from E* to C* and thus increases the initial velocity V_0. No such increase was observed in the actual experiment. If $k_1^* \ll k_{-1}^*$ and the equilibrium between E* and C* is in favor of E*, then for a significant formation of [T*] as observed experimentally, it would also require that $k_2^* \gg k_{-2}^* + k_3^*$ so that $[T^*]_\infty \gg [C^*]_\infty$. Under these conditions $1/\tau_1 = k_{-1}^* + k_2^*$ (see Appendix) which is much larger than $1/\tau_2 = k_1^* + k_{-2}^* + k_3^*$ (from eq 12). Since this is not the case (Table I), the C_2

Scheme IV: Possible Mechanisms Consistent with Experimental Results

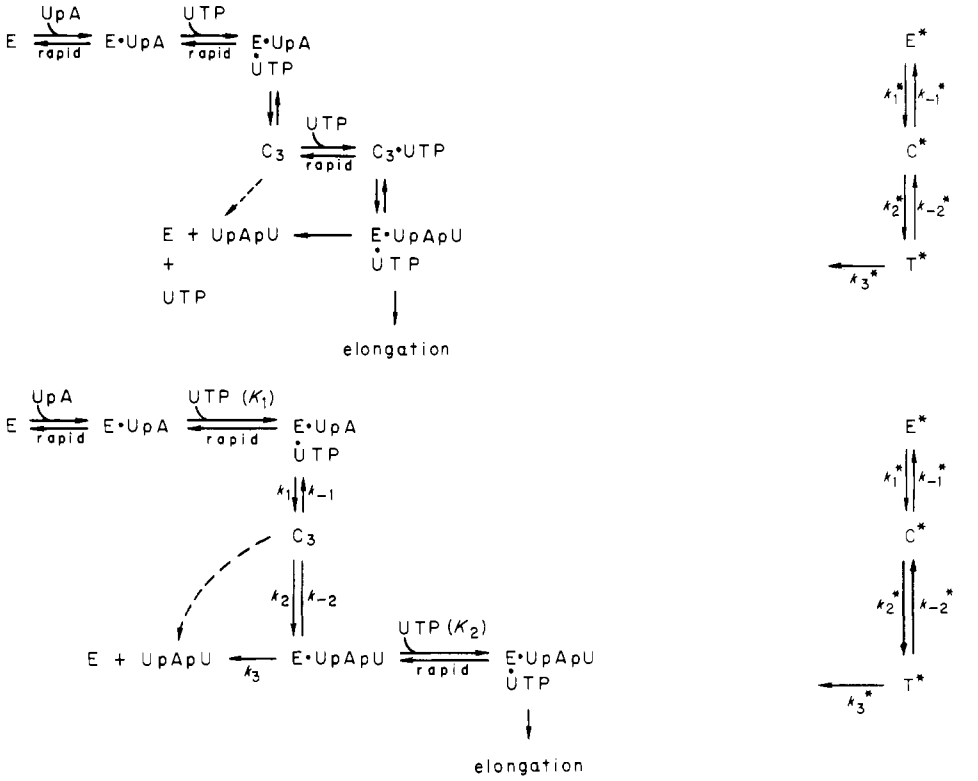

mechanism can also be excluded.

So far, only the C_3 mechanism still survives. In this mechanism, the conformational rearrangement of the E·UpA·UTP complex into C_3 is essential for subsequent formation of the phosphodiester bond. Alternatively, the phosphodiester bond formation may be completed at C_3 and the subsequent step may represent the conformational change of the E·UpApU complex (e.g., translocation) which is necessary for RNA chain elongation. A critical question may be raised here that since the effective rate constants are dependent on the substrate concentration, the two relaxation times derived for all the mechanisms shown in Scheme II could also be dependent on the substrate concentration. Thus, one must consider another important factor in elucidating the kinetic mechanism: the dependence of the rate of RNA chain initiation on the substrate concentrations.

Binding of an Additional UTP Molecule. The dependence of net [^{3}H]UMP incorporation into the initiation complex on the UTP concentration suggests binding of more than one UTP molecule to the enzyme–DNA complex during the initiation process (Shimamoto & Wu, 1980). This is further supported by the dependence of the total relaxation amplitude on the UTP concentration observed in the present study (Table I). Since the observed relaxation times are essentially independent of the UTP concentration, the binding of the additional UTP molecule should also be in a rapid equilibrium. Taking into account of both the number of the relaxation times and the stoichiometry of UTP binding, the minimal mechanism consistent with all the experimental observations must include at least three rapid binding processes (UpA and at least two UTP molecules) and two relatively slow steps corresponding to the two observed relaxation times. Nevertheless, all the discussions concerning the possible mechanisms of initiation presented above are still applicable since the concentration dependence of UTP has not entered into consideration for the mechanisms.

For the C_3 type mechanism, there are three possibilities that the binding of an additional UTP molecule may take place, either at E*, C*, or T*. In order to distinguish among these possibilities, let us consider the dependence of $[T^*]_\infty$ on the UTP concentration. By substituting τ_i's in eq 11 with k_i^*'s (see Appendix), one obtains

$$[T^*]_\infty = \frac{k_1^* k_2^* [E]_0}{(1/\tau_1)(1/\tau_2)} = \frac{k_1^* k_2^* [E]_0}{k_1^* k_2^* + k_3(k_1^* + k_{-1}^* + k_2^*) + k_{-2}^*(k_1^* + k_{-1}^*)} \quad (16)$$

The denominator of this equation is equal to $(1/\tau_2)(1/\tau_2)$ and thus is independent of the UTP concentration. Since the total amplitude, as represented by $[T^*]_\infty$, increases with increasing the UTP concentration, the term $k_1^* k_2^*$ in the numerator should also be increased. Note that the first term in the denominator is also $k_1^* k_2^*$. Since the total value of denominator remains unchanged as the concentration of UTP increases, the increase in the value of the first term in the denominator will be compensated by the decrease in the values of the second and/or the third terms. If the additional UTP binding takes place in E* (see the C_3 mechanism in Scheme III), only k_1^* would vary with the UTP concentration (but not other k_i^*'s) and the compensation among different terms in the denominator could not occur. This means that the denominator and, therefore, the product of the two relaxation times would be dependent on the UTP concentrations, which is apparently contradictory to the experimental results.

Possible Mechanisms Consistent with All the Data. Excluding all the mechanisms inconsistent with the experimental observations, we are left with only two C_3 mechanisms, in which binding of the additional UTP molecule occurs either at C* or T*. These mechanisms are depicted in Scheme IV. If the additional UTP molecule binds at C*, k_2^* and k_{-1}^* will become dependent on the UTP concentration [Scheme IV(a)]. Thus, increasing the concentration of UTP could lead to a decrease in k_{-1}^*, compensating for the increase of k_1^* and k_2^* (the concentration dependence of k_1^* is due to the binding of

Table III: Kinetic Parameters for the C_3 Mechanism in Scheme IV(a)

Intrinsic Rate Constant (s^{-1})

$k_1 = 20.3$ $k_{-1} = 3.21$ $k_2 = 23.6$ $k_{-2} = 0$ $k_3 = 14.9$

Dissociation Constants for UTP Binding

K_1 (first UTP) = 1.85×10^{-4} M

K_2 (second UTP) = 1.36×10^{-5} M

Relaxation Times and Amplitudes Calculated from Kinetic Parameters

[UpA]	[UTP] (μM)	τ_1 (ms)	τ_2 (ms)	$A_1 + A_2$ (nM)
saturating	100	42.8	97.8	16
saturating	10.8	44.8	102	2.8

first UTP molecule at E*). On the other hand, if the additional UTP binding is at T* [Scheme IV(b)], both k_{-2}* and k_3* could decrease by increasing the UTP concentration to compensate for the increase of k_1*. According to eq 12, the rates for the slow steps in both mechanisms cannot exceed $1/\tau_1 + 1/\tau_2 = 33$ s^{-1} (from Table I).

Irrespective of the exact location of binding, the additional UTP molecule acts as an activator or a discriminator in the catalytic pathway of RNA synthesis. It either facilitates the formation of initiation complex [Scheme IV(a)] or increases the stability of the initiation complex and thereby facilitates the elongation process [Scheme IV(b)]. Thus, the additional UTP binding may be crucial in driving the initiation reaction or in discriminating between the abortive or productive initiation pathways. The idea that more than one binding site may exist for UTP (or other nucleoside triphosphates) is in accord with previous reports that the steady-state RNA synthesis follows the Michaelis–Menten kinetics only when substrates are present in excess (Anthony et al., 1969; Downey & So, 1970). Lack of correlation between the inhibitions on RNA synthesis and the DNA-dependent pyrophosphate exchange reaction catalyzed by RNA polymerase also suggests multiple substrate binding sites on the enzyme (Slepneva et al., 1978).

The data that we have obtained from a real time analysis of the initiation of RNA synthesis by fast kinetic techniques indicate that the rate-determining steps in the initiations are unimolecular processes. This is contrary to the conclusion by Rhodes & Chamberlin (1974) based on their rifampicin challenge experiments that the rate-determining step in RNA chain initiation is the binding of initiator. The discrepancy between their conclusion and ours may be due to the invalid assumptions used in the rifampicin challenge assays as discussed in the preceding paper (Shimamoto & Wu, 1980) and by others (McClure & Cech, 1978).

The unimolecular processes involved in the initiation of RNA synthesis are represented by k_1* and k_2* in Scheme IV, which may be either the formation of the first phophodiester bond or the conformational rearrangement of the E·UpA·UTP complex or the initiation complex. The conformational rearrangement of initiation complexes could be the translocation of enzyme on the DNA template or the translocation of UpApU formed from the elongation site to the product terminus site on the enzyme (Krakow et al., 1976).

Finally, it should be emphasized that the mechanistic analysis presented in this paper is based on the two-exponential approximation of our kinetic data, the quality of which is insufficient to exclude the possibility of three or more relaxation times. However, even if better data were available, it would be very difficult to obtained reliable multiexponential analysis. The two mechanisms given in Scheme IV, therefore,

Scheme AI

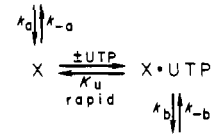

Scheme AII

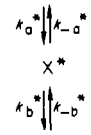

represent the minimal mechanisms of RNA chain initiation that are consistent with all our experimental observations. A set of kinetic parameters that fit the mechanism in Scheme IV(b) are listed in Table III. Further studies, of course, are required to distinguish between these two possible mechanisms.

Appendix

Derivation of Relaxation Times and Amplitudes for the Generalized Two-Step Mechanisms in Scheme II. By a phenomenological treatment (Shimamoto, 1976), all intermediates in a rapid equilibrium are grouped into one quasi-intermediate. With this treatment, one can analyze the kinetic data without handling the individual intermediates in a rapid equilibrium. For example, a UTP molecule binds rapidly to an intermediate, X, in a kinetic pathway to form X·UTP as shown in the reaction Schemes AI and AII. Since X and X·UTP are in a rapid equilibrium, a quasi-intermediate X* is denoted to represent the sum of these two intermediates. The effective rate constants k_i*'s associated with X* are defined so as to maintain the same reaction fluxes in Schemes AI and AII. Thus, the two effective rate constants for the breakdown of X*, k_{-a}* and k_b*, are defined as

$$k_{-a}^* = \frac{k_{-a}[X]}{[X^*]} = \frac{k_{-a}K_u}{K_u + [UTP]} \qquad \text{(A1a)}$$

$$k_b^* = \frac{k_b[X{\cdot}UTP]}{[X^*]} = \frac{k_b[UTP]}{K_u + [UTP]} \qquad \text{(A1b)}$$

where K_u is the dissociation constant for the X·UTP complex. From these equations, it can be seen that increasing the concentration of UTP will increase the value of k_b* and decrease the value of k_{-a}*. When UTP is in large excess, the free UTP concentration is equal to its total concentration. Under these conditions, Scheme AII becomes kinetically equivalent to Scheme AI. Therefore, from the concentration dependence of k_i*, the detailed mechanism involving the rapid equilibrium can be delineated.

Each of the four mechanisms shown in Scheme II can be described by a conservation equation

$$[E]_0 = [E^*] + [T^*] + [D^*] \text{ (or } [C^*]) \qquad \text{(A2)}$$

where $[E]_0$ is the total concentration of the active enzyme–DNA complex and two independent rate equations. For mechanism a (Scheme II), the two rate equations are

$$\frac{d[E^*]}{dt} = k_1^*[D^*] - (k_{-1}^* + k_2^*)[E^*] + k_{-2}^*[T^*] =$$

$$k_1^*E_0 - (k_1^* + k_{-1}^* + k_2^*)[E^*] + (k_{-2}^* - k_1^*)[T^*] \qquad \text{(A3)}$$

$$\frac{d[T^*]}{dt} = k_2^*[E^*] - k_{-2}^*[T^*] \qquad \text{(A4)}$$

These two linear first-order differential equations can be expressed by a matrix equation:

$$\frac{d}{dt}\begin{pmatrix}[E^*]\\[T^*]\end{pmatrix}=\begin{pmatrix}-k_1^*-k_{-1}^*-k_2^* & k_{-2}^*-k_1^*\\ k_2^* & -k_{-2}^*\end{pmatrix}\begin{pmatrix}[E^*]\\[T^*]\end{pmatrix}+\begin{pmatrix}k_1^*E_0\\0\end{pmatrix} \quad (A5)$$

The corresponding matrix equations for mechanisms b and c (Scheme II) are given by eq A6 and A7, respectively

$$\frac{d}{dt}\begin{pmatrix}[E^*]\\[T^*]\end{pmatrix}=\begin{pmatrix}-k_2^* & k_{-2}^*\\ k_2^*-k_{-1}^* & -k_1^*-k_{-1}^*-k_2^*\end{pmatrix}\begin{pmatrix}[E^*]\\[T^*]\end{pmatrix}+\begin{pmatrix}0\\k_1^*[E]_0\end{pmatrix} \quad (A6)$$

$$\frac{d}{dt}\begin{pmatrix}[C^*]\\[T^*]\end{pmatrix}=\begin{pmatrix}-k_1^*-k_{-1}^*-k_2^* & k_{-2}^*-k_1^*\\ k_2^* & -k_{-2}^*-k_3^*\end{pmatrix}\begin{pmatrix}[C^*]\\[T^*]\end{pmatrix}+\begin{pmatrix}k_1^*[E]_0\\0\end{pmatrix} \quad (A7)$$

Equations A5–A7 can be written in a general form

$$\frac{d}{dt}\begin{pmatrix}[A^*]\\[T^*]\end{pmatrix}=\begin{pmatrix}a_{11} & a_{12}\\ a_{21} & a_{22}\end{pmatrix}\begin{pmatrix}[A^*]\\[T^*]\end{pmatrix}+\begin{pmatrix}b_1\\b_2\end{pmatrix} \quad (A8)$$

where A* represents E* in mechanisms a and b and C* in mechanism c. The relaxation times τ_1 and τ_2 are found by solving the quadratic equation

$$\left(\frac{1}{\tau}\right)^2+(a_{11}+a_{22})\frac{1}{\tau}+a_{11}a_{22}-a_{12}a_{21}=0 \quad (A9)$$

The stationary concentration of T* can be expressed as

$$[T^*]_\infty=\frac{b_1a_{21}-b_2a_{11}}{a_{11}a_{22}-a_{12}a_{21}} \quad (A10)$$

From eq A5–A7, one obtains a common relationship for all four mechanisms:

$$b_1a_{21}-b_2a_{11}=k_1^*k_2^*[E]_0 \quad (A11)$$

It can be seen from eq A9 that

$$\frac{1}{\tau_1}\frac{1}{\tau_2}=a_{11}a_{22}-a_{12}a_{21} \quad (A12)$$

Substituting eq A11 and A12 into eq A10, one gets

$$[T^*]_\infty=k_1^*k_2^*\tau_1\tau_2[E]_0 \quad (A13)$$

Also from eq A9, one obtains

$$\frac{1}{\tau_1}+\frac{1}{\tau_2}=-(a_{11}+a_{22})=k_1^*+k_{-1}^*+k_2^*+k_{-2}^*(+k_3^*) \quad (A14)$$

If $k_{-1}^* \gg k_1^*$ and $k_2^* \gg k_{-2}^*+k_3^*$ in mechanism c, then $|a_{11}| \gg |a_{22}|$ and $|a_{11}| \gg |a_{12}|$ (obviously $|a_{11}| > |a_{21}|$). The discriminant for the solution of the quadratic equation A9 becomes

$$\begin{aligned}D&=[(a_{11}+a_{22})^2-4(a_{11}a_{22}-a_{12}a_{21})]^{1/2}\\&=|a_{11}+a_{22}|\left[1-4\frac{a_{11}a_{22}-a_{12}a_{21}}{(a_{11}+a_{22})^2}\right]^{1/2}\\&\simeq|a_{11}+a_{22}|\left[1-2\frac{a_{11}a_{22}-a_{12}a_{21}}{(a_{11}+a_{22})^2}\right]\\&=-(a_{11}+a_{22})+2\frac{a_{11}a_{22}-a_{12}a_{21}}{a_{11}+a_{22}}\\&\simeq-(a_{11}+a_{22})\end{aligned} \quad (A15)$$

Thus, the two relaxation times for mechanism c are

$$\begin{aligned}\frac{1}{\tau_1}&=\frac{1}{2}[-(a_{11}+a_{22})+D]\simeq-(a_{11}+a_{22})\\&=k_{-1}^*+k_2^*\\\frac{1}{\tau_2}&=\frac{1}{2}[-(a_{11}+a_{22})-D]\simeq-\frac{a_{11}a_{22}-a_{12}a_{21}}{a_{11}+a_{12}}\\&=k_1^*+k_{-2}^*+k_3^*\end{aligned} \quad (A16)$$

The conditions that $k_{-1}^* \gg k_1^*$ and $k_2^* \gg k_{-2}^*+k_3^*$, therefore, lead to $1/\tau_1 \gg 1/\tau_2$, which is contradictory to the experimental observation.

References

Anthony, D. D., Wu, C.-W., & Goldthwait, D. A. (1969) *Biochemistry 8*, 246–256.

Downey, K. M., & So, A. G. (1970) *Biochemistry 9*, 2520–2525.

Goldthwait, D. A., Anthony, D. D., & Wu, C.-W. (1970) in *Proceedings of the 1st International Lepetit Colloquium* (Silvestri, L., Ed.) p 10, North-Holland Publishing Co., Amsterdam.

Krakow, J. S., Rhodes, G., & Jovin, T. M. (1976) in *RNA Polymerase* (Losick, R., & Chamberlin, M., Eds.) pp 127–157, Cold Spring Harbor Laboratory, Cold Spring Harbor, NY.

McClure, W. R., & Cech, C. L. (1978) *J. Biol. Chem. 253*, 8949–8956.

Nath, K., & Hurwitz, J. (1974) *J. Biol. Chem. 249*, 2605–2215.

Rhodes, G., & Chamberlin, M. J. (1974) *J. Biol. Chem. 250*, 9112–9120.

Shimamoto, N. (1976) *J. Biochem. (Tokyo) 80*, 961–968.

Shimamoto, N., & Wu, C.-W. (1980) *Biochemistry* (preceding paper in this issue).

Slepneva, I. A., Zakharova, N. V., & Bucker, J. M. (1978) *FEBS Lett. 87*, 273–276.